International Journal of Advances in Engineering and Management (IJAEM)
Volume 5, Issue 8 Aug 2023, pp: 388-394 www.ijaem.net ISSN: 2395-5252

Deformation and Stability Analysis of a Semi-Excavated and Semi-Filled Slope in the Southern Region

Shen Quan[1], Zhang Cheng-li[1],
Zhang Yi-dan[1], Wang Chao-hui[1], Yan yuan[2]
[1]*College of civil engineering, Hunan University of Technology, Zhuzhou, Hunan, China,412001*
[2] *Hunan Automotive Engineering Vocational College,zhuzhou, China,412001*

Date of Submission: 10-08-2023 Date of Acceptance: 20-08-2023

ABSTRACT: Due to the constraints of terrain conditions and highway alignment, semi-excavated and semi-filled slope embankments are inevitable in the design and construction process. These structural forms of semi-excavated and semi-filled slope embankments disrupt the original equilibrium stability of rock and soil slopes, making them susceptible to geological hazards such as collapse and landslides under the influence of construction and operation. In this study, based on field reconnaissance data, the stability of high semi-excavated and semi-filled slope embankments was investigated using numerical simulation methods. The research results indicate that without anchor rod support, the toe slope of the high semi-excavated and semi-filled slope embankment exhibits a bulging deformation, with a maximum displacement of 0.2959 meters. After introducing an anchor rod framework support, the maximum deformation of the slope is 9.946e-2, only one-third of the unsupported condition. The safety factor of the slope after the implementation of anchor rods is 1.184, which is an 18.2% increase compared to the case without anchor rod support, indicating improved slope stability and safety. The research findings provide reference for the construction and design of semi-excavated and semi-filled slope embankments.

KEYWORDS:Half Digging and half filling; High slope; Deformation; Stability; bolt

Ⅰ. INTRODUCTION

The terrain of the mountainous and hilly areas traversed by a certain southern expressway is complex and unique. Due to the constraints of terrain conditions and highway alignment, semi-excavated and semi-filled slope embankments are inevitable in the design and construction process. Moreover, many semi-excavated sections involve deep excavation, and many semi-filled sections involve high embankments. These structural forms of deep excavation and high embankment slope embankments disrupt the original equilibrium stability of rock and soil slopes. Under the influence of construction and operation, they are prone to geological hazards such as collapse and landslides. These hazards can damage road embankments, bridges, culverts, lead to traffic accidents, and cause casualties, resulting in significant losses to human life and property safety, and posing great harm to the expressway transportation infrastructure.

Due to the differences in the physical and mechanical properties of geological formations on both sides of the semi-excavated and semi-filled embankment, as well as variations in internal structure and settlement time, instability of embankment slopes in the filling area or uneven settlement along interfaces pose challenging engineering problems that hinder the performance and safety of the embankment. In the study of the stability of semi-excavated and semi-filled embankments, most researchers focus on the excavation-filling interface, analyzing its influence on the overall embankment[1-3]. JIANG Chong et al. [4]determined the thickness and safety thickness of karst region embankment cave roofs based on the engineering characteristics of cave roofs in karst areas. Liu Longqi et al. [5]summarized the composition and mechanical properties of slope accumulation materials and discussed common embankment distress caused by slope instability. Tang Xinlei et al. [6] analyzed the working mechanisms of insulation installation, embedded heating rods, and ventilation pipe installation, comparing their advantages and disadvantages. Li Qun, Sun Xufeng et al.[7]analyzed

International Journal of Advances in Engineering and Management (IJAEM)
Volume 5, Issue 8 Aug 2023, pp: 388-394 www.ijaem.net ISSN: 2395-5252

the reinforcement mechanism and failure mode of embankments, and based on this, considering the setting of a series of steps at the excavation-filling interface, established a reasonable embankment stability analysis model. This model fully considers the effects of step interfaces and the reinforcement of rock and soil materials, using the limit equilibrium method to solve the stability coefficient. Finally, a comparative analysis was conducted with engineering examples. The results showed that the addition of steps and geosynthetic materials significantly improved the embankment's resistance to sliding. Liu Jianlei, Nai Lei et al.[8]pointed out that the stability of semi-excavated and semi-filled embankments is controlled by various factors such as the structural type of the excavation-filling interface and rock conditions. Through sensitivity analysis, it was found that fill height, groundwater, and cohesive strength of fill are sensitive factors affecting embankment stability. Su Yonghua, Xie Zhiyong et al. [9] analyzed a semi-excavated and semi-filled embankment interface of a certain highway and combined orthogonal experimental design, statistical methods, and Msarma method to form a mechanical mechanism analysis method for the stability of the interface. The first four factors studied were cohesion, internal friction angle, interface, and foundation inclination. Su Yonghua, Luo Zhengdong et al. [10]proposed that the grey relational analysis method is applicable to the analysis and evaluation of complex and uncertain problems in the stability of embankment slopes in mountainous areas. They improved the traditional grey relational analysis method. Combining the advantages of uniform experimental design, they established a uniform experimental analysis method for the stability of embankment slopes in mountainous areas based on improved grey relational degree. Taking a semi-excavated and semi-filled highway in mountainous areas as an example, they analyzed the influencing factors of deformation stability and strength stability of embankment slopes. Xia Yingzhi [11]started from the factors influencing the stability of semi-excavated and semi-filled embankments and used PLAXIS finite element software to conduct numerical simulation studies on the influence of embankment fill height on slope stability. It was pointed out that with the increase of fill height, incremental displacement gradually shifts from the outer side of the fill embankment to the inner side.

In summary, this unique embankment form has not yet been thoroughly researched and contains many unknowns in various aspects. Without systematic exploration and understanding of the deformation and stability characteristics of this specific embankment type, there are many risks in practical construction and operation. Therefore, this paper, based on field reconnaissance data, uses numerical simulation methods to study the stability of high semi-excavated and semi-filled slope embankments, aiming to provide some reference for engineering construction and operation.

Ⅱ. PROJECT OVERVIEW

The contract section 4 of a certain southern expressway starts from chainage K24+425 and ends at chainage K29+500 for the mainline, and includes branch line from DZK2+985 to DZK4+000. The total length of the route is 6.09 kilometers, with 3 mainline bridges totaling 2938 meters and 5 interchange ramp bridges totaling 1525 meters. There are 12 culverts in the project, with a total excavation volume of 2.4 million cubic meters and a total fill volume of 1.08 million cubic meters. The project has a total duration of 26 months.

Within this contract section, the mainline route consists mainly of four lanes, designed for a speed of 100 km/h. The standard cross-section of the embankment has a width of 26 meters. This includes a lane width of 2×(2×3.75) meters, a hard shoulder width of 2×3.0 meters (including a right side shoulder width of 2×0.5 meters), a soft shoulder width of 2×0.75 meters, and a median width of 3.5 meters (including a median shoulder width of 2×0.75 meters).

The project starts southeast of Mount Yinnashan and east of Tongguzhang, extends in a southeasterly direction along the Han River, crosses the Fenghuang Mountains, skirts the southwestern corner of the Tangxi Reservoir, and reaches the northern part of the Hanjiang Plain in Raoping County, Chaozhou City. Influenced by the joint effects of northwest and northeast trending fault structures, the project area exhibits a typical structural and erosional landform. The predominant landform types in the project area are mountains and hills, with some portions located within the Chao-Shan Plain.

Ⅲ. ANALYSIS OF DEFORMATION AND STABILITY OF TYPICAL CROSS-SECTION SLOPE IN DEEP EXCAVATION

The research focuses on a typical deep excavation road embankment slope section of a certain highway. To simplify the analysis, a representative model of a semi-cut semi-fill slope in deep excavation is constructed as shown in Figure 1. The relevant parameter values are presented in Table 1：

International Journal of Advances in Engineering and Management (IJAEM)
Volume 5, Issue 8 Aug 2023, pp: 388-394 www.ijaem.net ISSN: 2395-5252

Figure 1(Model of Semi-Cut Semi-Fill Slope)

Soil and Rock Types	Compressibility Modulus(MPa)	Density (g/cm³)	Cohesion (kPa)	Internal Friction Angle (°)	Poisson's Ratio	Liquid Limit	Plastic Limit
Silty Clay	6.5	1.8	16	18	0.35	35.4	23
Sandy Silty Clay	6.5	1.8	22	25	0.3	36	24
Completely Weathered Granite	15	1.75	20	20	0.3	32.3	21.6
Intensely Weathered Granite (Semi-Rock Semi-Soil State)	18	2.2	30	35	0.3	30.2	20.3
Intensely Weathered Granite (Fragmented State)	18	2.2	30	30	0.3	30.2	20.3
Gravelly Soil	5.49	1.83	6.5	26.9	0.3	19.7	14.6
Moderately Weathered Granite	300	2.5			0.25		
Framework	25000						
Anchor Bolt	200000						

Table 1(Material Parameter Table)

From top to bottom, the layered materials are sandy silty clay, completely weathered granite, intensely weathered granite (semi-rock semi-soil state), and intensely weathered granite (fragmented state). The model dimensions are as follows: slope levels 1, 2, and 3 have a ratio of 1:1, while the following three levels have a ratio of 1:1.25. Each slope level has a height of 10 meters, and the platform width for the third level is 10 meters, while the rest are 2 meters. The uppermost layer of sandy silty clay is 8 meters thick, followed by a 7-meter thickness of completely weathered granite in the second layer. The third layer consists of intensely weathered granite (semi-rock semi-soil state) and has a thickness of 15 meters. Below that, there is intensely weathered granite (fragmented state).

The model is constrained in the X-direction on both sides and in the XY-direction on the lower side. The grid division size is 1 meter, using a free division method and neutral axis algorithm. The model is divided into 13,295 grids. The calculated total displacement cloud map is shown in the figure below.

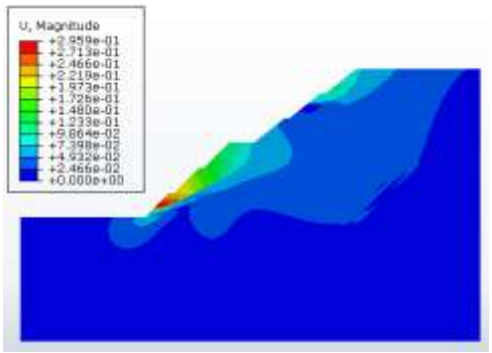

Figure 2(Total Displacement Cloud Map)

International Journal of Advances in Engineering and Management (IJAEM)
Volume 5, Issue 8 Aug 2023, pp: 388-394 www.ijaem.net ISSN: 2395-5252

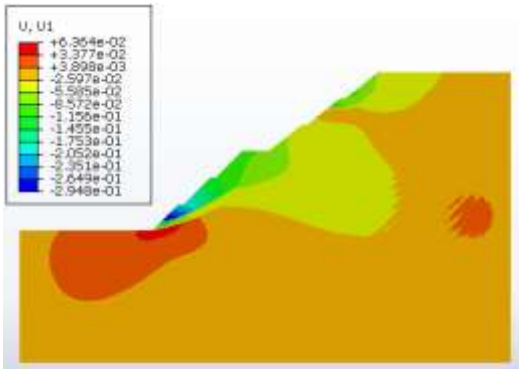

Figure 3(Horizontal Displacement Map)

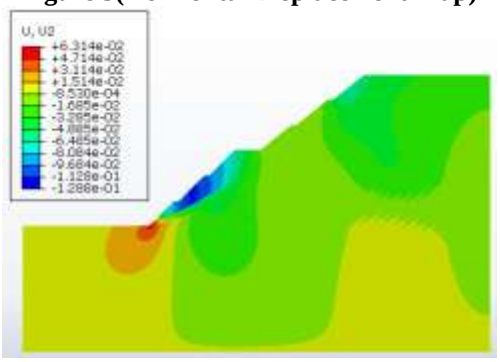

Figure 4(Vertical Displacement Cloud Map)

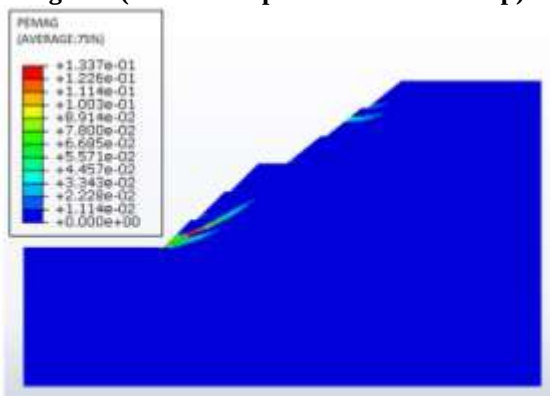

Figure 5(Plastic Deformation Map)

The slope begins to slide from the center of the Level 1 slope. The entire Level 2 slope moves downward, causing an uplift at the base of the slope and resulting in significant uneven deformation of the embankment. The maximum displacement of the slope is 0.2959 meters, located in the middle of the Level 1 slope. The displacement cloud map indicates the presence of two sliding surfaces within the slope. The deformation is larger and more critical along the sliding surface at the base of the slope, requiring reinforcement measures to prevent excessive deformation.

There are two zones of plastic deformation observed in the slope. They initiate from the base of the Level 1 slope and the middle of the Level 5 slope, with the maximum plastic deformation reaching 1.337e-1, located within the interior of the Level 1 slope. Due to the steepness of the first three levels of the slope and its height of 60 meters, instability and failure are likely. Hence, protective measures need to be implemented to restrict the development of the plastic deformation zones.

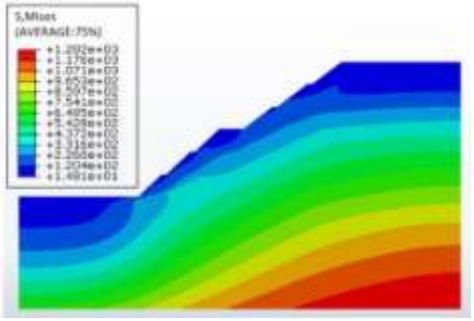

Figure 6(Soil Pressure Contour Map)

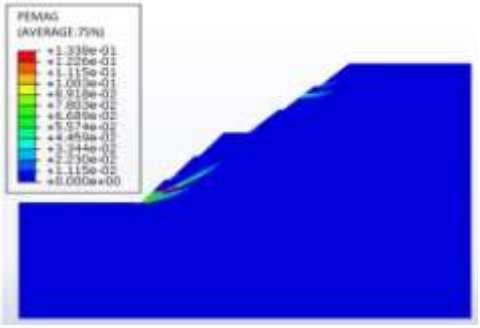

Figure 7(Plastic Deformation Contour Map atUltimate State)

By applying strength reduction, the slope's ultimate equilibrium condition is obtained by calculating until non-convergence. Under the equilibrium condition, plastic deformation is present, and the slope has two plastic deformation zones along sliding surfaces. Although these zones are not fully connected, excessive plastic deformation causes the software calculation to not converge. This yields a safety factor of 1.002 for the slope, indicating susceptibility to instability and failure under adverse conditions.At the ultimate state, plastic deformation reaches 0.1338. The slope experiences significant deformation due to sliding along the base's sliding surface, leading to instability and failure. Therefore, it's necessary to implement reinforcement measures to strengthen the slope through supportive measures.

Ⅳ. ANALYSIS OF REINFORCEMENT EFFECTS OF ANCHORED FRAME BEAMS ON SEMI-CUT SEMI-FILL HIGH SLOPES

Given that theoretical calculations might not reflect the deformation of slopes reinforced with anchorages, finite element analysis is employed to

International Journal of Advances in Engineering and Management (IJAEM)
Volume 5, Issue 8 Aug 2023, pp: 388-394 www.ijaem.net ISSN: 2395-5252

evaluate the reinforcement effects of anchored frame beams on semi-cut semi-fill high slopes. The anchored frame beam model with anchor rods is as follows:

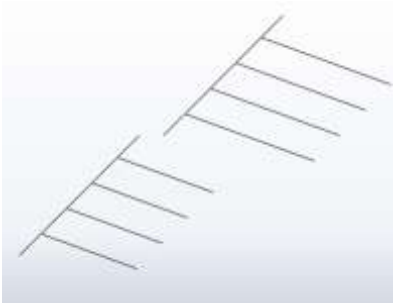

Figure 8(Anchor Rod Frame System Model)

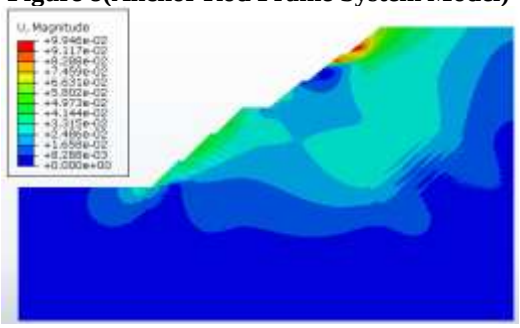

Figure 9(Total Displacement Contour Map)

Based on the design drawing, the anchor rods are inclined at an angle of 20 degrees from the horizontal and are embedded into the bottom two layers of the slope soil. The upper anchor rod has a length of 11.5 meters, while the lower anchor rod has a length of 8.5 meters. Both anchor rods have a diameter of 28mm. The frame section measures 0.3 meters by 0.3 meters and is constructed using poured concrete. The anchor rods are represented using truss elements, while the frame is modeled using beam elements. The resulting displacement cloud maps include the total displacement, vertical displacement, horizontal displacement, and plastic deformation maps, as shown in the following figures.

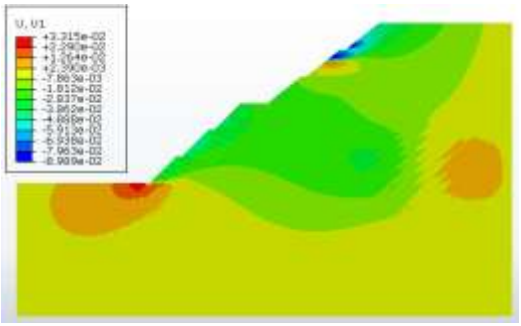

Figure 10: Horizontal Displacement Contour Map

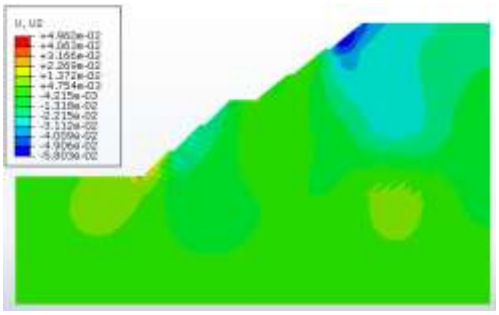

Figure 11: Vertical DisplacementContour Map

The displacement cloud map reveals that due to the effect of the anchor rod frame, the development of sliding surfaces at the base of the slope is obstructed. No sliding surface is formed at the base of the slope. The slope displacement transforms into a shared deformation between the slope and the anchor rod frame system. As a result, the slope deformation is significantly reduced to only 9.946e-2, which is one-third of the deformation without anchored support. Additionally, the maximum displacement is transferred to the upper part of the Level 5 slope, enhancing slope stability.According to the horizontal displacement cloud map, the maximum horizontal displacement is transferred to the upper-middle part of the Level 5 slope and is smaller compared to the case without anchor rods. The vertical displacement cloud map indicates that embankment uplift is reduced, leading to significant improvement in the uneven settlement caused by slope deformation.

According to the simplified slope model, the ABAQUS software was used to calculate the minimum safety factor using the method of strength reduction. The basic principle of the strength reduction method involves reducing the strength parameters of the slope fill material. This reduction is achieved by dividing both the cohesion (c) and the internal friction angle (α) by a reduction factor (Fs), resulting in a new set of strength parameters. These new parameters are then used for calculations, and the slope is analyzed repeatedly until the critical failure state is reached. The reduction factor (Fs) at this point becomes the safety factor. The expression for strength reduction is as follows:

$$c_t = \frac{c}{F_S} \quad (1)$$

$$\alpha_T = \arctan\left(\frac{\alpha}{F_s}\right) \quad (2)$$

Compared to the Swedish Method of Slices, the strength reduction method offers several advantages. It doesn't require assuming the shape of the potential sliding surface in advance. It dynamically displays the yielding and failure processes of the slope, considering the actual stress state of the slope. It can identify the potential sliding

International Journal of Advances in Engineering and Management (IJAEM)
Volume 5, Issue 8 Aug 2023, pp: 388-394 www.ijaem.net ISSN: 2395-5252

surface (potential displacement curve) and the trend of shear stress increment. In its displacement cloud map, potential sliding scenarios of the slope can be directly observed, along with the corresponding safety factors.For a reduction factor ($F_S = 1$), the plastic deformation contour map is shown in Figure 12. From the graph, it can be observed that the plastic zone at the lower part of the slope has not developed into a sliding surface. The maximum plastic deformation is also only one-third of that without support. The slope deformation is constrained by the anchor rods, transferring it to the deeper soil layers. The effect of the frame constrains surface deformation, enhancing the overall stability and safety of the slope.

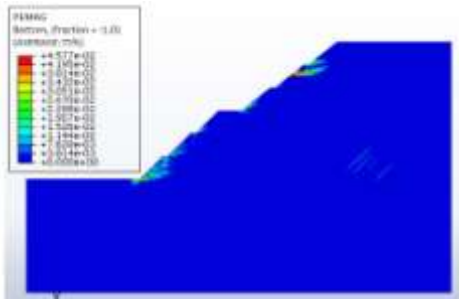

Figure 12: Plastic Deformation Contour Map

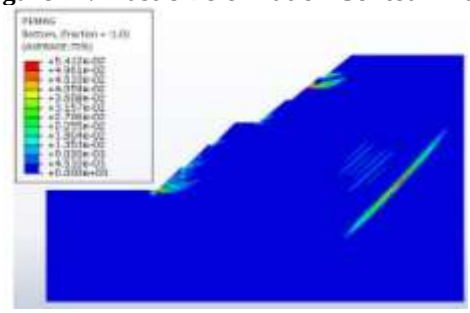

Figure 13: Plastic Deformation Contour Map with Safety Factor of 1.05

The plastic deformation contour map for a reduction factor ($F_S = 1.05$) is shown in Figure 13. From the above figure, it can be observed that when the reduction factor is 1.05, the plastic zone at the base of the slope begins to develop beyond the length of the anchor rods. A large plastic zone appears in the deeper layers of the slope, accompanied by smaller plastic zones. The upper part of the slope has a broader development area for plastic zones, resulting in larger deformations.The plastic deformation contour map for a reduction factor($F_S = 1.1$)is shown in Figure 14. From the graph, it's evident that the plastic zone at the base of the slope develops from the Level 1 slope to the deep area of the anchor rod influence zone of the Level 1 slope, and then extends to the Level 2 slope. The plastic deformation in the deeper layers of the slope becomes increasingly significant, while the development of the plastic zone in the upper part of the slope is less pronounced.

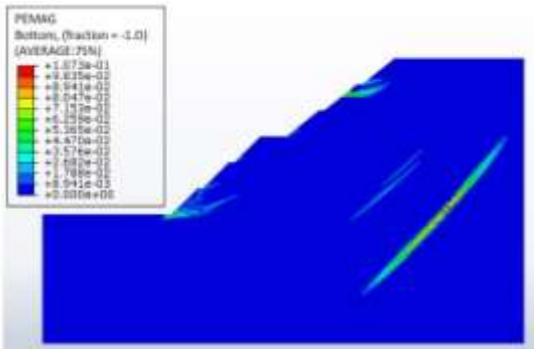

Figure 14: Plastic Deformation Contour Map with Reduction Factor of 1.1

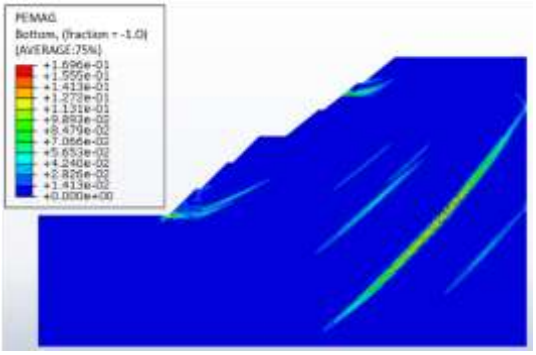

Figure 15: Plastic Deformation Contour Mapwith Reduction Factor of 1.185

The plastic deformation contour map for a reduction factor($F_S = 1.184$) (limit equilibrium state) is shown in Figure 15. From the figure, it's evident that at the limit state, the plastic zone at the base of the slope develops up to the Level 3 slope. The plastic zone is located behind the anchor rod influence zone, and the sliding surface shifts to deeper layers compared to the case without support. The length of the deformation zone in the deeper layers of the slope reaches the slope height, and multiple longer plastic zones appear.The determination of whether the slope is safe or not is based on whether the plastic zones are continuous. Therefore, it can be concluded that the safety factor of the slope reinforced with anchor rods is 1.184, which is 18.2% higher compared to the case without anchor rods. This indicates that the slope is safer after being reinforced with anchor rods.

V. CONCLUSION

1）Without anchor rod support, the lower part of the semi-cut semi-fill high slope experiences uplift deformation at the base of the slope. The maximum

displacement is 0.2959 meters, located in the middle of the Level 1 slope. The slope exhibits two sliding surfaces, with greater deformation occurring along the sliding surface at the base of the slope. The safety factor of the slope is 1.002, indicating susceptibility to instability and failure under adverse conditions.

2）With the introduction of anchor rod frame support, the development of sliding surfaces at the base of the slope is hindered due to the effect of the anchored frame beams. As a result, no sliding surfaces are formed at the slope base. The slope deformation transforms into a shared deformation between the slope and the anchored frame beam system. The maximum deformation of the slope is 9.946e-2, only one-third of the deformation without anchor rod support. Additionally, the maximum displacement is transferred to the upper part of the Level 5 slope, enhancing the slope's stability. The deformation of the slope is significantly improved.The maximum plastic deformation is also only one-third of that without support. The slope deformation is constrained by the anchor rods, transferring the deformation to the deeper soil layers. After the implementation of anchor rod support, the safety factor of the slope increases to 1.184, which is 18.2% higher compared to the case without anchor rod support. This enhancement in safety indicates that the slope becomes more stable and secure.

Without anchor rod support, the lower part of the semi-cut semi-fill high slope experiences uplift deformation at the base of the slope. The maximum displacement is 0.2959 meters.

After introducing anchor rod frame support, the maximum deformation of the slope is reduced to 9.946e-2, which is only one-third of the deformation without anchor rod support. Furthermore, the safety factor of the slope increases to 1.184 with anchor rod support, representing an improvement of 18.2% compared to the case without anchor rod support. This indicates that the slope becomes significantly safer after the implementation of anchor rod support.

REFERENCES

[1] WAN Qi, YAN Changgen, ZHANG Xiaoming, et al. Model 'Test on the Half-Filled and Half-Excavated Subgradein Loess Area[J].Journal of Chongqing Jiaotong University(Natural Science),2022,41(12):99-103+133.

[2] FU Jing,MAO Xuesong,WU Qian, et al. Instability Mechanism of a Cut-and-fill Subgrade Along a River[J].China Sciencepaper,2022,17(10):1099-1104.

[3] KOU Zhentao. Analysis of Foundation deformation and failure mechanism and Treatment in semi-filling and semi-excavating sites of loess area[D].Chang'an University, 2019.

[4] JIANG Chong, ZHAO Minghua, CAO Wengui. Stability analysis of subgrade cave roofs in karst region[J]. J. Cent. South Univ, 2008,15:38-44.

[5] LIU Longqi, MAO Xuesong, WANG Liyun,et al.Stability Analysis Based on the Full fill Subgrade of Slope Product Section: 5th International Conference on Civil Engineering and Transportation, 2015.

[6] TANG Xinlei, MAO Xuesong, TANG Ke. Analysis of Advantages and Disadvantages of Stability Measures in Permafrost Subgrade: 3rd International Conference on Advances in Materials, Mechatronics and Civil Engineering, 2018.

[7] LI Qun,SUN Xufeng. Analysis on the Stablity of Part-cut and Part-fill Embankment with Reinforced Geogrid[J].Highway Engineering, 2008(03):117-119.

[8] LU Jianlei,NAI Lei,XI Xiaohong. Analysis of sensitive factor on the stability of cut and filled subgrade[J].Joumal of China and Foreign Highway, 2009,29(2):26-28.

[9] SU Yonghua,XIE Zhiyong,XU Nengxiong, et al. Mechanism analysis of stability of cut-and-fill roadbed interface[J].Rock and Soil Mechanics, 2010,31(2):497-502.

[10] SU Yonghua，LUO Zhengdong，Ll Xiang. Gray correlation analysis method for cut-and-fill roadbed slope stabilitybased on uniform experiment[J]. Rock and Soil Mechanics, 2012,33(8):2259-2264.

[11] XIA Yingzhi.Simulation Study on Stability of Semi-filled and Semi-excavatedSubgrade of a First Grade Highway[J].Highway Engineering, 2019,44(3):92-96, 137.